



Synthesis and reactivity of ruthenium complexes with 1,1'-dithiolate ligands

Fang-Hui Wu^{a,b}, Taike Duan^a, Lude Lu^b, Qian-Feng Zhang^{a,*}, Wa-Hung Leung^c

^a Institute of Molecular Engineering and Applied Chemistry, Anhui University of Technology, 59 Hudong Road, Ma'anshan, Anhui 243002, PR China

^b Material Chemistry Laboratory, Nanjing University of Science and Technology, Nanjing 210094, PR China

^c Department of Chemistry, The Hong Kong University of Science and Technology, Clear Water Bay, Kowloon, Hong Kong, PR China

ARTICLE INFO

Article history:

Received 6 March 2009

Received in revised form 20 April 2009

Accepted 21 April 2009

Available online 3 May 2009

Keywords:

Ruthenium

Sulfur

1,1'-Dithiolate

Phosphine

Synthesis

Crystal structure

ABSTRACT

Reactions of $[\text{Ru}(\text{PPh}_3)_3\text{Cl}_2]$ with ROCS_2K in THF at room temperature and at reflux gave the kinetic products *trans*- $[\text{Ru}(\text{PPh}_3)_2(\text{S}_2\text{COR})_2]$ ($\text{R} = {}^n\text{Pr}$ **1**, ${}^i\text{Pr}$ **2**) and the thermodynamic products *cis*- $[\text{Ru}(\text{PPh}_3)_2(\text{S}_2\text{COR})_2]$ ($\text{R} = {}^n\text{Pr}$ **3**, ${}^i\text{Pr}$ **4**), respectively. Treatment of $[\text{RuHCl}(\text{CO})(\text{PPh}_3)_3]$ with ROCS_2K in THF afforded $[\text{RuH}(\text{CO})(\text{S}_2\text{COR})(\text{PPh}_3)_2]$ ($\text{R} = {}^n\text{Pr}$ **5**, ${}^i\text{Pr}$ **6**) as the sole isolable products. Reaction of $[\text{RuCl}_2(\text{PPh}_3)_3]$ with tetramethylthiuram disulfide $[\text{Me}_2\text{NCS}_2]_2$ gave a Ru(III) dithiocarbamate complex, $[\text{Ru}(\text{PPh}_3)_2(\text{S}_2\text{CNMe}_2)_2\text{Cl}_2]$ (**7**). This reaction involved oxidation of ruthenium(II) to ruthenium(III) by the disulfide group in $[\text{Me}_2\text{NCS}_2]_2$. Treatment of **7** with 1 equiv. of $[\text{M}(\text{MeCN})_4][\text{ClO}_4]$ ($\text{M} = \text{Cu}, \text{Ag}$) gave the stable cationic ruthenium(III)-alkyl complexes $[\text{Ru}\{\text{C}(\text{NMe}_2)\text{QC}(\text{NMe}_2)\text{S}\}(\text{S}_2\text{CNMe}_2)(\text{PPh}_3)_2][\text{ClO}_4]$ ($\text{Q} = \text{O}$ **8**, S **9**) with ruthenium-carbon bonds. The crystal structures of complexes **1**, **2**, **4**- CH_2Cl_2 , **6**, **7**- $2\text{CH}_2\text{Cl}_2$, **8**, and **9**- $2\text{CH}_2\text{Cl}_2$ have been determined by single-crystal X-ray diffraction. The ruthenium atom in each of the above complexes adopts a pseudo-octahedral geometry in an electron-rich sulfur coordination environment. The 1,1'-dithiolate ligands bind to ruthenium with bite S-Ru-S angles in the range of 70.14(4)–71.62(4)°. In **4**- CH_2Cl_2 , the P-Ru-P angle for the mutually *cis* PPh_3 ligands is 103.13(3)°, the P-Ru-P angles for other complexes with mutually *trans* PPh_3 ligands are in the range of 169.41(4)–180.00(6)°. The alkylcarbamate $[\text{C}(\text{NMe}_2)\text{QC}(\text{NMe}_2)\text{S}]^-$ ($\text{Q} = \text{O}, \text{S}$) ligands in **8** and **9** are planar and bind to the ruthenium centers via the sulfur and carbon atoms from the C=S and N=C double bonds, respectively. The Ru-C bond lengths are 1.975(5) and 2.018(3) Å for **8** and **9**- $2\text{CH}_2\text{Cl}_2$, respectively, which are typical for ruthenium(III)-alkyl complexes. Spectroscopic properties along with electrochemistry of all complexes are also reported in the paper.

© 2009 Published by Elsevier B.V.

1. Introduction

Transition metal-sulfur complexes are of significance because of diverse bonding possibilities and their roles in homogeneous catalysis [1]. Of particular interest are ruthenium-sulfur complexes that may serve as functional models for Fe-S proteins due to the periodic relationship between ruthenium and iron [2]. In recent years there has been an increasing interest in ruthenium complexes with sulfur-donor ligands, in part because of the high catalytic activity of RuS_2 in various hydrotreating processes [3]. It may be thus understood that a number of organometallic and classical coordination complexes of ruthenium with thiolate and dithio acids (R_2NCS_2^- , ROCS_2^- , RCS_2^- , R_2PS_2^- and $(\text{RO})_2\text{PS}_2^-$) have been synthesized and their reactivity investigated [4–6]. For example, the reaction of $[\text{Ru}(\text{PPh}_3)_3\text{Cl}_2]$ with alkaline salts of 1,1-dithiolates gave the complexes $[\text{Ru}(\text{S},\text{S})_2(\text{PPh}_3)_2]$ which have the phosphines mutually *cis* [4]. The reported type *cis*- $[\text{Ru}(\text{S},\text{S})_2(\text{PPh}_3)_2]$ complexes include *cis*- $[\text{Ru}(\text{S}_2\text{CNR}_2)_2(\text{PPh}_3)_2]$ ($\text{R} = \text{Me}, \text{Et}, {}^n\text{Pr}, {}^i\text{Pr}$) [7–9], *cis*-

$[\text{Ru}(\text{S}_2\text{COR})_2(\text{PPh}_3)_2]$ ($\text{R} = \text{Et}, {}^i\text{Pr}$) [10], *cis*- $[\text{Ru}(\text{S}_2\text{P}(\text{OEt})_2)_2(\text{PPh}_3)_2]$ [11], *cis*- $[\text{Ru}(\text{S}_2\text{CSC}_2\text{Ph}_2)_2(\text{PPh}_3)_2]$ [12] and *cis*- $[\text{Ru}(\text{S}_2\text{CSC}_5\text{H}_4)_2(\text{PPh}_3)_2]$ [13]. Charavorty and coworkers have studied the redox properties of these complexes and found that a coordination rearrangement along with the redox process occurs in oxidation-induced *cis*-*trans* isomerization of these complexes [14]. It was found that the preferred geometry is *cis* for ruthenium (II) and *trans* for ruthenium(III) [15]. The *cis* to *trans* isomerization process in the ruthenium species $[\text{Ru}(\text{S}_2\text{CO}^i\text{Pr})_2(\text{PPh}_3)_2]^{0/+}$ has recently been re-investigated by Takagi and coworkers [10]. Electrochemical oxidation at various concentrations of PPh_3 in the bulk solution gives both complexes *cis*- $[\text{Ru}(\text{S}_2\text{CO}^i\text{Pr})_2(\text{PPh}_3)_2]$ with d^6 -ruthenium(II) and *trans*- $[\text{Ru}(\text{S}_2\text{CO}^i\text{Pr})_2(\text{PPh}_3)_2]^+$ with d^5 -ruthenium(III) have been isolated and structurally characterized. As a matter of fact, the formation of the *cis*- $[\text{Ru}(\text{S},\text{S})_2(\text{PPh}_3)_2]$ complexes strongly supports the *cis* stereochemistry predicted for the starting compound. Remarkably, with a less bulky phosphine ligand, PMe_2Ph , the *trans* isomers *trans*- $[\text{Ru}(\text{S}_2\text{COEt})_2(\text{PMe}_2\text{Ph})_2]$ [16] and *trans*- $[\text{Ru}(\text{S}_2\text{PEt}_2)_2(\text{PMe}_2\text{Ph})_2]$ [17] with d^6 -ruthenium(II) centers were isolated. However, the ruthenium complexes with dithio ligands have been relatively less explored. In efforts to develop

* Corresponding author. Tel./fax: +86 555 2312041.
E-mail address: zhangqf@ahut.edu.cn (Q.-F. Zhang).

ruthenium-1,1'-dithiolate-based complexes for redox catalysis [18,19], we sought to investigate the reaction chemistry, e.g. oxidation reactions and structural variation, of ruthenium-sulfur complexes. We report here the synthesis, reactivity, and crystal structures of the ruthenium complexes with the 1,1'-dithiolate ligands ROCS_2^- and R_2NCS_2^- ($\text{R} = \text{Me}$, ^nPr , ^iPr).

2. Experimental

2.1. General

All synthetic manipulations were carried out under dry nitrogen by standard Schlenk techniques. Solvents were purified, distilled and degassed by standard methods. $[\text{Ru}(\text{PPh}_3)_3\text{Cl}_2]$ [20], $[\text{RuHCl}(\text{CO})(\text{PPh}_3)_3]$ [21], $[\text{Cu}(\text{MeCN})_4][\text{ClO}_4]$ [22] were prepared according to the literature methods. $[\text{Ag}(\text{MeCN})_4][\text{ClO}_4]$ was obtained from the reaction of Ag_2O and HClO_4 in MeCN solution. Potassium xanthates ROCS_2K ($\text{R} = \text{Pr}$ and ^iPr) were synthesized from the reactions of CS_2 and KOH in ROH. Tetramethylthiuram disulfide was purchased from Alfa Ltd. and used as received. NMR spectra were recorded on a Bruker ALX 300 spectrometer operating at 300 and 121.5 MHz for ^1H and ^{31}P , respectively. Chemical shifts (δ , ppm) were reported with reference to SiMe_4 (^1H) and H_3PO_4 (^{31}P). Infrared spectra (KBr) were recorded on a Perkin-Elmer 16 PC FT-IR spectrophotometer. Cyclic voltammetry was performed with on a CHI 660 electrochemical analyzer. A standard three-electrode cell was used with glassy carbon working electrode, a platinum counter electrode and Ag/AgCl reference electrode under an nitrogen atmosphere at 25 °C. Formal potentials (E°) were measured in CH_2Cl_2 solutions with 0.1 M $[\text{Bu}_4\text{N}]\text{PF}_6$ as supporting electrolyte and reported with reference to the ferrocenium-ferrocene couple ($\text{Cp}_2\text{Fe}^{+/0}$). In the -1.5 to $+1.2$ V region, a potential scan rate of 100 mV s^{-1} was used. Elemental analyses were carried out using a Perkin-Elmer 2400 CHN analyzer.

2.2. Synthesis of *trans*- $[\text{Ru}(\text{PPh}_3)_2(\text{S}_2\text{COR})_2]$ ($\text{R} = ^n\text{Pr}$ **1**, ^iPr **2**)

A mixture of $[\text{Ru}(\text{PPh}_3)_3\text{Cl}_2]$ (144 mg, 0.15 mmol) and 2 equiv. of $^n\text{PrOCS}_2\text{K}$ (53 mg, 0.30 mmol) or $^i\text{PrOCS}_2\text{K}$ (53 mg, 0.30 mmol) in THF (20 mL) was stirred at room temperature for 2 h. The solvent was pumped off and the residue was recrystallized from $\text{CH}_2\text{Cl}_2/\text{Et}_2\text{O}$ at -10 °C to give orange crystalline solids in two days. For **1**: Yield: 63 mg, 45%. ^1H NMR (300 MHz, CDCl_3): δ 1.12 (t, 6H, $-\text{CH}_3$), 2.38 (m, 4H, $-\text{CH}_2-$), 4.48 (t, 4H, $-\text{CH}_2\text{O}-$), 7.02–7.28 (m, 30H, $-\text{C}_6\text{H}_5$) ppm. $^{31}\text{P}\{^1\text{H}\}$ NMR (121.5 MHz, CDCl_3): δ 46.8 (s) ppm. IR (KBr, cm^{-1}): 1637 (vs), 1244 (vs), 1096 (s), 1040 (m), 741 (m), 697 (s), 536 (m), 520 (m). Anal. Calc. for $\text{C}_{44}\text{H}_{44}\text{O}_2\text{P}_2\text{S}_4\text{Ru}$: C, 59.0; H, 4.95. Found: C, 58.7; H, 4.91%. For **2**: Yield: 56 mg, 41%. ^1H NMR (300 MHz, CDCl_3): δ 1.15–2.24 (m, 12H, $-\text{CH}_3$), 5.14 (m, 2H, $-\text{CH}-$), 7.08–7.26 (m, 30H, $-\text{C}_6\text{H}_5$) ppm. $^{31}\text{P}\{^1\text{H}\}$ NMR (121.5 MHz, CDCl_3): δ 45.7 (s) ppm. IR (KBr, cm^{-1}): 1635 (vs), 1241 (vs), 1093 (s), 1042 (m), 744 (m), 690 (s), 546 (m), 522 (m). Anal. Calc. for $\text{C}_{44}\text{H}_{44}\text{O}_2\text{P}_2\text{S}_4\text{Ru}$: C, 59.0; H, 4.95. Found: C, 58.3; H, 4.94%.

2.3. Synthesis of *cis*- $[\text{Ru}(\text{PPh}_3)_2(\text{S}_2\text{COR})_2]$ ($\text{R} = ^n\text{Pr}$ **3**, ^iPr **4**)

A mixture of $[\text{Ru}(\text{PPh}_3)_3\text{Cl}_2]$ (144 mg, 0.15 mmol) and 2 equiv. of $^n\text{PrOCS}_2\text{K}$ (53 mg, 0.30 mmol) or $^i\text{PrOCS}_2\text{K}$ (53 mg, 0.30 mmol) in THF (20 mL) was heated at reflux for 2 h. The solvent was pumped off and the residue was recrystallized from $\text{CH}_2\text{Cl}_2/\text{Et}_2\text{O}$ to give red crystalline solids in a week. For **3**: Yield: 89 mg, 64%. ^1H NMR (300 MHz, CDCl_3): δ 0.97 (t, 6H, $-\text{CH}_3$), 2.15 (m, 4H, $-\text{CH}_2-$), 4.22 (t, 4H, $-\text{CH}_2\text{O}-$), 7.11–7.26 (m, 30H, $-\text{C}_6\text{H}_5$) ppm. $^{31}\text{P}\{^1\text{H}\}$ NMR (121.5 MHz, CDCl_3): δ 39.2 (s) ppm. IR (KBr, cm^{-1}): 1639 (vs),

1241 (vs), 1094 (s), 1043 (m), 745 (m), 693 (s), 540 (m), 521 (m). Anal. Calc. for $\text{C}_{44}\text{H}_{43}\text{O}_2\text{P}_2\text{S}_4\text{Ru}\cdot(\text{CH}_2\text{Cl}_2)$: C, 55.1; H, 4.63. Found: C, 54.7; H, 4.61%. For **4**: Yield: 77 mg, 55%. ^1H NMR (300 MHz, CDCl_3): δ 1.13–2.28 (m, 12H, $-\text{CH}_3$), 5.15 (m, 2H, $-\text{CH}-$), 7.01–7.27 (m, 30H, $-\text{C}_6\text{H}_5$) ppm. $^{31}\text{P}\{^1\text{H}\}$ NMR (121.5 MHz, CDCl_3): δ 38.4 (s) ppm. IR (KBr, cm^{-1}): 1631 (vs), 1238 (vs), 1091 (s), 1046 (m), 745 (m), 692 (s), 543 (m), 518 (m). Anal. Calc. for $\text{C}_{44}\text{H}_{43}\text{O}_2\text{P}_2\text{S}_4\text{Ru}\cdot(\text{CH}_2\text{Cl}_2)$: C, 55.1; H, 4.63. Found: C, 54.6; H, 4.58%.

2.4. Synthesis of $[\text{RuH}(\text{CO})(\text{PPh}_3)_2(\text{S}_2\text{COR})]$ ($\text{R} = ^n\text{Pr}$ **5**, ^iPr **6**)

A mixture of $[\text{RuHCl}(\text{CO})(\text{PPh}_3)_3]$ (150 mg, 0.16 mmol) and $^n\text{PrOCS}_2\text{K}$ (28 mg, 0.16 mmol) or $^i\text{PrOCS}_2\text{K}$ (28 mg, 0.16 mmol) was dissolved in THF (20 mL) and then stirred overnight at room temperature. A color change from yellow to pale orange was observed. The solvent was pumped off and the residue was washed with hexane and further recrystallized from $\text{CH}_2\text{Cl}_2/\text{hexane}$. Yellow block crystals of **5** or **6** were obtained in three days. For **5**: Yield: 72 mg, 52%. ^1H NMR (300 MHz, CDCl_3): δ 0.89 (t, 3H, $-\text{CH}_3$), 1.57 (s, 1H, RuH), 2.27 (m, 2H, $-\text{CH}_2-$), 2.81–3.14 (m, 2H, $-\text{CH}_2\text{O}-$), 7.33–7.61 (m, 30H, $-\text{C}_6\text{H}_5$) ppm. $^{31}\text{P}\{^1\text{H}\}$ NMR (121.5 MHz, CDCl_3): δ 41.4 (s) ppm. IR (KBr, cm^{-1}): 1935 (vs), 1636 (vs), 1237 (vs), 1090 (s), 1038 (m), 738 (m), 694 (s), 536 (m), 523 (m). Anal. Calc. for $\text{C}_{41}\text{H}_{38}\text{O}_2\text{P}_2\text{S}_2\text{Ru}$: C, 62.3; H, 4.85. Found: C, 61.6; H, 4.82%. For **6**: Yield: 69 mg, 50%. ^1H NMR (300 MHz, CDCl_3): δ 0.93 (t, 6H, $-\text{CH}_3$), 1.63 (s, 1H, RuH), 5.12 (m, 4H, $-\text{CH}_2-$), 7.29–7.63 (m, 30H, $-\text{C}_6\text{H}_5$) ppm. $^{31}\text{P}\{^1\text{H}\}$ NMR (121.5 MHz, CDCl_3): δ 40.6 (s) ppm. IR (KBr, cm^{-1}): 1942 (vs), 1634 (vs), 1232 (vs), 1085 (s), 1034 (m), 741 (m), 696 (s), 542 (m), 528 (m). Anal. Calc. for $\text{C}_{41}\text{H}_{38}\text{O}_2\text{P}_2\text{S}_2\text{Ru}$: C, 62.3; H, 4.85. Found: C, 62.1; H, 4.79%.

2.5. Synthesis of $[\text{Ru}(\text{S}_2\text{CNMe}_2)(\text{PPh}_3)_2\text{Cl}_2]\cdot 2\text{CH}_2\text{Cl}_2$ (**7**)

To a solution of $[\text{Ru}(\text{PPh}_3)_3\text{Cl}_2]$ (144 mg, 0.15 mmol) in THF (20 mL) at 0 °C was added tetramethylthiuram disulfide (24 mg, 0.10 mmol), and the mixture was stirred overnight at room temperature. The resulting green solution was evaporated to dryness, and the residue was recrystallized from $\text{CH}_2\text{Cl}_2/\text{hexane}$ to give dark green crystals. Yield: 56 mg, 43%. FT-IR (KBr, cm^{-1}): 1531 (vs), 1434 (s), 1106 (s), 997 (s), 910 (m), 741 (w), 694 (s), 595 (m), 520 (s). $\mu_{\text{eff}} = 1.91 \mu_{\text{B}}$ at 296 K. Anal. Calc. for $\text{C}_{39}\text{H}_{36}\text{NCl}_2\text{P}_2\text{S}_2\text{Ru}\cdot 2(\text{CH}_2\text{Cl}_2)$: C, 49.9; H, 4.09; N, 1.42. Found: C, 49.5; H, 4.01; N, 1.44%.

2.6. Synthesis of $[\text{Ru}\{\text{C}(\text{NMe}_2)\text{OC}(\text{NMe}_2)\text{S}\}(\text{S}_2\text{CNMe}_2)(\text{PPh}_3)_2][\text{ClO}_4]$ (**8**)

To a solution of complex **7** (82 mg, 0.01 mmol) in CH_2Cl_2 (10 mL) was added a solution of $[\text{Cu}(\text{MeCN})_4][\text{ClO}_4]$ (33 mg, 0.10 mmol) in MeCN (3 mL), and the mixture was stirred for 4 h at room temperature. The crude product was filtered out and washed with hexane. Deep green crystals of **8** were obtained by recrystallization of the crude product from $\text{CH}_2\text{Cl}_2/\text{Et}_2\text{O}$ in a week. Yield: 44 mg, 57%. FT-IR (KBr, cm^{-1}): 1594 (vs), 1395 (m), 1167 (s), 1098 (s), 1157 (m), 986 (m), 747 (m), 696 (s), 632 (m), 589 (m), 523 (s), 408 (s). $\mu_{\text{eff}} = 1.92 \mu_{\text{B}}$ at 296 K. Anal. Calc. for $\text{C}_{45}\text{H}_{48}\text{N}_3\text{O}_5\text{ClP}_2\text{S}_3\text{Ru}$: C, 53.7; H, 4.81; N, 4.18. Found: C, 52.9; H, 4.76; N, 4.14%.

2.7. Synthesis of $[\text{Ru}\{\text{C}(\text{NMe}_2)\text{SC}(\text{NMe}_2)\text{S}\}(\text{S}_2\text{CNMe}_2)(\text{PPh}_3)_2][\text{ClO}_4]\cdot 2\text{CH}_2\text{Cl}_2$ (**9**)

To a solution of complex **7** (82 mg, 0.10 mmol) in CH_2Cl_2 (15 mL) was added a solution of $[\text{Ag}(\text{MeCN})_4][\text{ClO}_4]$ (38 mg, 0.10 mmol) in MeCN (3 mL), and the mixture was stirred for 0.5 h at room temperature. The solvent was pumped off and the residue was washed with hexane and further recrystallized from $\text{CH}_2\text{Cl}_2/\text{Et}_2\text{O}$. Brown green crystals were obtained in three days.

Yield: 38 mg, 49%. FT-IR (KBr, cm^{-1}): 1591 (vs), 1397 (m), 1156 (m), 1094 (s), 989 (m), 751 (m), 700 (s), 585 (m), 526 (s), 451 (w), 405 (s). $\mu_{\text{eff}} = 1.94 \mu_{\text{B}}$ at 296 K. Anal. Calc. for $\text{C}_{45}\text{H}_{48}\text{N}_3\text{O}_4\text{ClP}_2\text{S}_4\text{Ru} \cdot 2(\text{CH}_2\text{Cl}_2)$: C, 47.4; H, 4.40; N, 3.53. Found: C, 47.2; H, 4.37, N, 3.52%.

2.8. X-ray crystallography

Crystallographic data and experimental details for **1**, **2**, **4**· CH_2Cl_2 , and **6** in Table 1 and for **7**· $2\text{CH}_2\text{Cl}_2$, **8**, and **9**· $2\text{CH}_2\text{Cl}_2$ in Table 2 are summarized. Intensity data were collected on a Bruker SMART APEX 2000 CCD diffractometer using graphite-monochromated Mo K α radiation ($\lambda = 0.71073 \text{ \AA}$) at 293(2) K. The collected frames were processed with the software SAINT [23]. The data was corrected for absorption using the program SADABS [24]. Structures were solved by the direct methods and refined by full-matrix least-squares on F^2 using the SHELXTL software package [25]. All non-hydrogen atoms were refined anisotropically. The positions of all hydrogen atoms were generated geometrically ($C_{\text{sp}^3}\text{-H} = 0.96$ and $C_{\text{sp}^2}\text{-H} = 0.93 \text{ \AA}$), assigned isotropic thermal parameters, and allowed to ride on their respective parent carbon or nitrogen atoms before the final cycle of least-squares refinement. The CH_2Cl_2 solvent molecule in **7**· $2\text{CH}_2\text{Cl}_2$ was isotropically refined without hydrogen atoms due to disorder. The four oxygen atoms of the $[\text{ClO}_4]^-$ anion in **8** were isotropically refined. One of the CH_2Cl_2 solvent molecules in **9**· $2\text{CH}_2\text{Cl}_2$ was isotropically refined with hydrogen atoms.

3. Results and discussion

Interaction of $[\text{Ru}(\text{PPh}_3)_3\text{Cl}_2]$ with $^n\text{PrOCS}_2\text{K}$ or $^i\text{PrOCS}_2\text{K}$ in THF at room temperature for 2 h followed by recrystallization from $\text{CH}_2\text{Cl}_2/\text{Et}_2\text{O}$ at $-10 \text{ }^\circ\text{C}$ gave *trans*- $[\text{Ru}(\text{PPh}_3)_2(\text{S}_2\text{COR})_2]$ ($\text{R} = ^n\text{Pr}$ **1**, ^iPr **2**) as the sole isolable products, whereas the same reactions carried out in refluxing solvent afforded *cis*- $[\text{Ru}(\text{PPh}_3)_2(\text{S}_2\text{COR})_2]$ ($\text{R} = ^n\text{Pr}$ **3**, ^iPr **4**) only. It appears that reaction of $[\text{Ru}(\text{PPh}_3)_3\text{Cl}_2]$ with ROCS_2K initially gave the kinetic products *trans*- $[\text{Ru}(\text{PPh}_3)_2(\text{S}_2\text{COR})_2]$, which crystallized quickly at a relatively lower tempera-

ture. With longer reaction time and at higher temperature at $80 \text{ }^\circ\text{C}$, *trans*- $[\text{Ru}(\text{PPh}_3)_2(\text{S}_2\text{COR})_2]$ isomerized to the thermodynamic products *cis*- $[\text{Ru}(\text{PPh}_3)_2(\text{S}_2\text{COR})_2]$. The course of reaction between $[\text{Ru}(\text{PPh}_3)_3\text{Cl}_2]$ and $^n\text{PrOCS}_2\text{K}$ was followed by ^{31}P NMR spectroscopy. Initially, only one resonance peak at 46.8 ppm due to the *trans* complex was found for the reaction mixture. After the solution was allowed to stand for 1 day under heating condition, a new ^{31}P signal at 39.2 ppm probably attributable to *cis* complex appeared. The ^{31}P NMR resonance for the *trans* complex shows a single peak downfield from that of the *cis* complex. The *cis* to *trans* isomerization process in the ruthenium species $[\text{Ru}(\text{S}_2\text{CO}^i\text{Pr})_2(\text{PPh}_3)_2]^{0/+}$ was induced by the oxidation reaction, which led to the formation of *trans*- $[\text{Ru}(\text{S}_2\text{CO}^i\text{Pr})_2(\text{PPh}_3)_2]^+$ with d^5 -ruthenium(III) [10]. Treatment of *cis*- $[\text{Ru}(\text{S}_2\text{COEt})_2(\text{PPh}_3)_2]$ with less bulky PMe_2Ph gave *trans*- $[\text{Ru}(\text{S}_2\text{COEt})_2(\text{PMe}_2\text{Ph})_2]$ [16], which is the first example of Ru(II) bis(xanthate) complex with a *trans* geometry. The present *trans*- $[\text{Ru}(\text{PPh}_3)_2(\text{S}_2\text{COR})_2]$ ($\text{R} = ^n\text{Pr}$ **1**, ^iPr **2**) complexes can be successfully isolated on the basis of thermodynamics. This is the first synthetic route to *trans*-bis(xanthate) complexes of ruthenium(II) by way of controlling reaction conditions.

The solid-state structures of *trans*-complexes **1** and **2** have been established by X-ray crystallography, as shown in Figs. 1 and 2. The corresponding selected bond lengths and angles are compiled in Table 3 for comparison. Both **1** and **2** crystallized in the monoclinic system, space group $P2_1/n$, with the ruthenium atom occupying a special position (0, 0, 0) imposing molecular centrosymmetry. The arrangement around the ruthenium in each complex shows the distorted octahedral coordination geometry. The two mutually *trans* xanthate ligands chelate the ruthenium atom with very acute bite angles of $71.62(4)^\circ$ for **1** and $71.55(4)^\circ$ for **2**, which compare well with those in *trans*- $[\text{Ru}(\text{S}_2\text{COEt})_2(\text{PMe}_2\text{Ph})_2]$ ($72.04(3)^\circ$) [16] and *trans*- $[\text{Ru}(\text{S}_2\text{COEt})_2(\text{PPh}_3)_2][\text{PF}_6]$ ($73.20(10)^\circ$) [10]. The two *trans* four-membered CS_2Ru rings across the central ruthenium atom are approximately planar with deviations of 0.001 \AA for **1** and 0.026 \AA for **2** from the least-squares plane, which induce distortions from idealized octahedral geometry. The $\text{Ru}^{\text{II}}\text{-S}$ bond lengths in both **1** and **2** are in the range of $2.4005(10)$ – $2.4139(9) \text{ \AA}$, which are comparable to those in *trans*- $[\text{Ru}(\text{S}_2\text{COEt})_2(\text{PPh}_3)_2]$ ($2.4005(10)$ – $2.4139(9) \text{ \AA}$) [10].

Table 1
Crystallographic data and experimental details for *trans*- $[\text{Ru}(\text{S}_2\text{COPr})_2(\text{PPh}_3)_2]$ (**1**), *trans*- $[\text{Ru}(\text{S}_2\text{COiPr})_2(\text{PPh}_3)_2]$ (**2**), *cis*- $[\text{Ru}(\text{S}_2\text{CO}^i\text{Pr})_2(\text{PPh}_3)_2] \cdot \text{CH}_2\text{Cl}_2$ (**4**· CH_2Cl_2), and $[\text{Ru}(\text{CO})(\text{S}_2\text{CO}^i\text{Pr})(\text{PPh}_3)_2]$ (**6**).

| Compound | 1 | 2 | 4 · CH_2Cl_2 | 6 |
|--|---|---|--|---|
| Empirical formula | $\text{C}_{44}\text{H}_{44}\text{O}_2\text{P}_2\text{S}_4\text{Ru}$ | $\text{C}_{44}\text{H}_{44}\text{O}_2\text{P}_2\text{S}_4\text{Ru}$ | $\text{C}_{45}\text{H}_{45}\text{O}_2\text{Cl}_2\text{P}_2\text{S}_4\text{Ru}$ | $\text{C}_{41}\text{H}_{38}\text{O}_2\text{P}_2\text{S}_2\text{Ru}$ |
| Formula weight | 896.04 | 896.04 | 979.96 | 789.84 |
| Crystal system | Monoclinic | Monoclinic | Triclinic | Triclinic |
| <i>a</i> (Å) | 10.4987(6) | 10.8517(10) | 10.9818(1) | 9.1934(3) |
| <i>b</i> (Å) | 8.8821(5) | 9.1682(8) | 12.3131(2) | 12.3641(4) |
| <i>c</i> (Å) | 22.1439(12) | 21.3852(19) | 17.6605(2) | 17.5218(6) |
| α (°) | | | 99.400(1) | 78.870(2) |
| β (°) | 95.995(3) | 99.273(7) | 94.139(1) | 75.762(2) |
| γ (°) | | | 102.634(1) | 74.672(2) |
| <i>V</i> (Å ³) | 2053.6(2) | 2099.8(3) | 2284.45(5) | 1844.28(11) |
| Space group | $P2_1/n$ | $P2_1/n$ | $P\bar{1}$ | $P\bar{1}$ |
| <i>Z</i> | 2 | 2 | 2 | 2 |
| <i>D</i> _{calc} (g cm ⁻³) | 1.449 | 1.417 | 1.425 | 1.442 |
| Temperature (K) | 296(2) | 296(2) | 296(2) | 296(2) |
| <i>F</i> (0 0 0) | 924 | 924 | 1006 | 812 |
| μ (Mo K α) (mm ⁻¹) | 0.700 | 0.684 | 0.749 | 0.660 |
| Total reflection | 18 929 | 19 197 | 42 432 | 25 173 |
| Independent reflection | 4684 | 4849 | 10384 | 8419 |
| <i>R</i> _{int} | 0.0770 | 0.0908 | 0.0427 | 0.0853 |
| <i>R</i> ₁ ^a , <i>wR</i> ₂ ^b (<i>I</i> > 2 σ (<i>I</i>)) | 0.0503, 0.1003 | 0.0597, 0.1158 | 0.0409, 0.1008 | 0.0554, 0.1053 |
| <i>R</i> ₁ , <i>wR</i> ₂ (all data) | 0.0675, 0.1182 | 0.0634, 0.1425 | 0.0551, 0.1090 | 0.0616, 0.1291 |
| GOF ^c | 0.995 | 0.974 | 1.024 | 0.954 |

^a $R_1 = \sum ||F_o| - |F_c|| / \sum |F_o|$.

^b $wR_2 = [\sum w(|F_o|^2 - |F_c|^2)|^2 / \sum w|F_o|^2]^{1/2}$.

^c $\text{GOF} = [\sum w(|F_o| - |F_c|)^2 / (N_{\text{obs}} - N_{\text{param}})]^{1/2}$.

Table 2

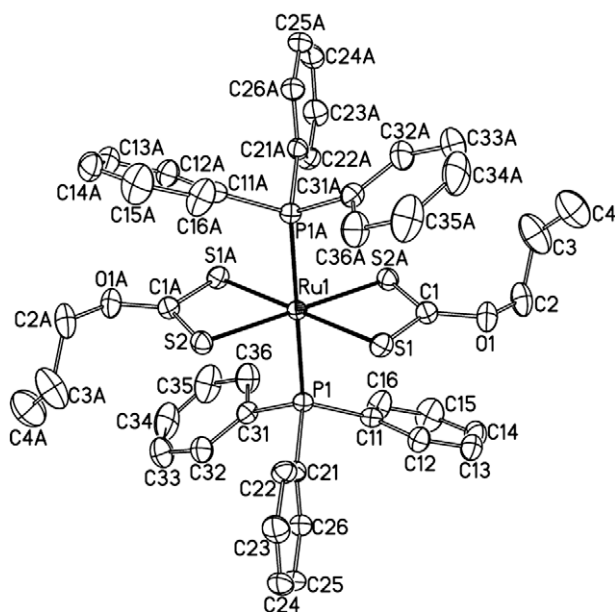
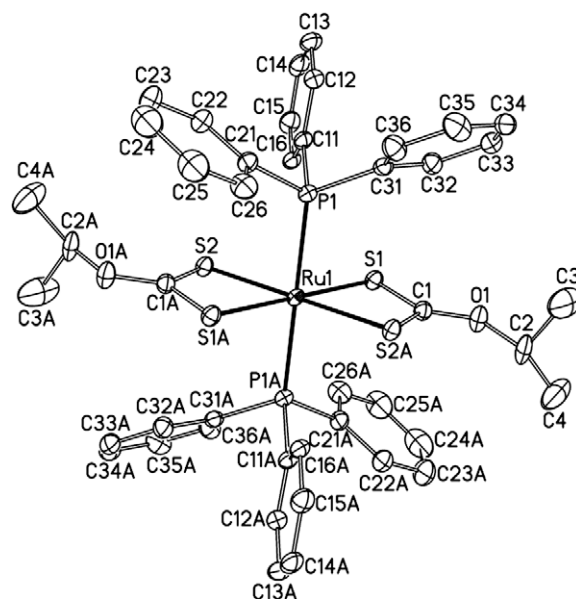
Crystallographic data and experimental details for $[\text{Ru}(\text{PPh}_3)_2(\text{S}_2\text{CNMe}_2)\text{Cl}_2] \cdot 2\text{CH}_2\text{Cl}_2$ ($7 \cdot 2\text{CH}_2\text{Cl}_2$), $[\text{Ru}(\text{SCNMe}_2\text{OCNMe}_2)(\text{S}_2\text{CNMe}_2)(\text{PPh}_3)_2][\text{ClO}_4]$ (**8**), and $[\text{Ru}(\text{SCNMe}_2\text{SCNMe}_2)(\text{S}_2\text{CNMe}_2)(\text{PPh}_3)_2][\text{ClO}_4] \cdot 2\text{CH}_2\text{Cl}_2$ ($9 \cdot 2\text{CH}_2\text{Cl}_2$).

| Compound | $7 \cdot 2\text{CH}_2\text{Cl}_2$ | 8 | $9 \cdot 2\text{CH}_2\text{Cl}_2$ |
|--|---|---|--|
| Empirical formula | $\text{C}_{41}\text{H}_{40}\text{NCl}_6\text{P}_2\text{S}_2\text{Ru}$ | $\text{C}_{45}\text{H}_{48}\text{N}_3\text{O}_5\text{ClP}_2\text{S}_3\text{Ru}$ | $\text{C}_{47}\text{H}_{52}\text{N}_3\text{O}_4\text{Cl}_5\text{P}_2\text{S}_4\text{Ru}$ |
| Formula weight | 986.57 | 1005.50 | 1191.42 |
| Crystal system | Monoclinic | Monoclinic | Triclinic |
| <i>a</i> (Å) | 10.3275(2) | 10.0643(5) | 11.5807(3) |
| <i>b</i> (Å) | 27.5603(4) | 19.3298(10) | 13.1583(3) |
| <i>c</i> (Å) | 15.5786(3) | 24.9177(12) | 18.7521(4) |
| α (°) | | | 78.151(1) |
| β (°) | 94.996(1) | 101.65(1) | 74.477(1) |
| γ (°) | | | 82.801(1) |
| <i>V</i> (Å ³) | 4417.28(14) | 4747.6(4) | 2687.08(11) |
| Space group | $P2_1/n$ | $P2_1/c$ | $P\bar{1}$ |
| <i>Z</i> | 4 | 4 | 2 |
| <i>D</i> _{calc} (g cm ⁻³) | 1.483 | 1.407 | 1.437 |
| Temperature (K) | 296(2) | 296(2) | 296(2) |
| <i>F</i> (0 0 0) | 2004 | 2072 | 1220 |
| μ (Mo K α) (mm ⁻¹) | 0.915 | 0.632 | 0.632 |
| Total reflection | 42 434 | 32 939 | 49 832 |
| Independent reflection | 10 112 | 9999 | 12 264 |
| <i>R</i> _{int} | 0.0321 | 0.0663 | 0.0139 |
| <i>R</i> ₁ ^a , <i>wR</i> ₂ ^b (<i>I</i> > 2 σ (<i>I</i>)) | 0.0487, 0.1247 | 0.0571, 0.0712 | 0.0412, 0.1172 |
| <i>R</i> ₁ , <i>wR</i> ₂ (all data) | 0.0674, 0.1355 | 0.0669, 0.0840 | 0.0479, 0.1247 |
| GOF ^c | 1.014 | 0.914 | 1.022 |

$$^a R_1 = \sum ||F_o| - |F_c|| / \sum |F_o|.$$

$$^b wR_2 = [\sum w(|F_o|^2 - |F_c|^2)^2 / \sum w|F_o|^2]^{1/2}.$$

$$^c \text{GOF} = [\sum w(|F_o| - |F_c|)^2 / (N_{\text{obs}} - N_{\text{param}})]^{1/2}.$$

**Fig. 1.** Perspective view of *trans*- $[\text{Ru}(\text{S}_2\text{COPr})_2(\text{PPh}_3)_2]$ **1**.**Fig. 2.** Perspective view of *trans*- $[\text{Ru}(\text{S}_2\text{CO}^i\text{Pr})_2(\text{PPh}_3)_2]$ **2**.

$\text{COEt}_2(\text{PMe}_2\text{Ph})_2]$ (2.380(2)–2.404(2) Å) [16], but longer than the $\text{Ru}^{\text{III}}\text{--S}$ bond lengths in *trans*- $[\text{Ru}(\text{S}_2\text{COEt})_2(\text{PPh}_3)_2][\text{PF}_6]$ (2.361(2)–2.373(2) Å). This difference may be taken as the difference in the ionic radii for ruthenium(II) and ruthenium(III). The Ru–P bond lengths (2.3557(9) Å for **1** and 2.3577(12) Å for **2**) fall in the usual range for ruthenium(II) complexes with PPh_3 ligands, but slightly longer than those in *trans*- $[\text{Ru}(\text{S}_2\text{COEt})_2(\text{PMe}_2\text{Ph})_2]$ (2.336(2) Å) [16] and $[\text{Ru}(\text{S}_2\text{PEt}_2)_2(\text{PMe}_2\text{Ph})_2]$ (2.252(2)–2.261(2) Å) [17].

The solid-state structure of $4 \cdot \text{CH}_2\text{Cl}_2$ has been determined by X-ray crystallography, as shown in Fig. 3. The corresponding selected bond lengths and angles are listed in Table 4. Similar complexes such as *cis*- $[\text{Ru}(\text{S}_2\text{COEt})_2(\text{PPh}_3)_2]$ [10,14], *cis*- $[\text{Ru}(\text{S}_2\text{CNEt}_2)_2(\text{PPh}_3)_2]$ [7] and *cis*- $[\text{Ru}(\text{S}_2\text{P}(\text{OEt})_2)_2(\text{PPh}_3)_2]$ [11] with *cis* geometry have

been reported. The neutral molecule is mononuclear with an octahedral geometry. The two PPh_3 ligands bind to the ruthenium center with the P–Ru–P angle of 103.13(3)°, and the two chelating $^i\text{PrOCS}_2^-$ ligands coordinate with the ruthenium with small bite angles (S–Ru–S angle of av. 71.55(3)°). The four-membered RuS_2P rings are approximately planar. Each ring contains a pair of long and short Ru–S bonds [Ru(1)–S(2) = 2.4593(8) Å (“long”) with Ru(1)–S(1) = 2.3839(7) Å (“short”); Ru(1)–S(3) = 2.4556(7) Å (“long”) with Ru(1)–S(4) = 2.3964(7) Å (“short”)]. The Ru–S bond lengths in $4 \cdot \text{CH}_2\text{Cl}_2$ (av. 2.4238(7) Å) is comparable to that in *cis*- $[\text{Ru}(\text{S}_2\text{P}(\text{OEt})_2)_2(\text{PPh}_3)_2]$ (av. 2.424(2) Å) with chelated dithiosphate ligands [11], but slightly longer than those in *cis*- $[\text{Ru}(\text{S}_2\text{CNEt}_2)_2(\text{PPh}_3)_2]$ (av. 2.3952(5) Å) with chelated dithiocarbamate

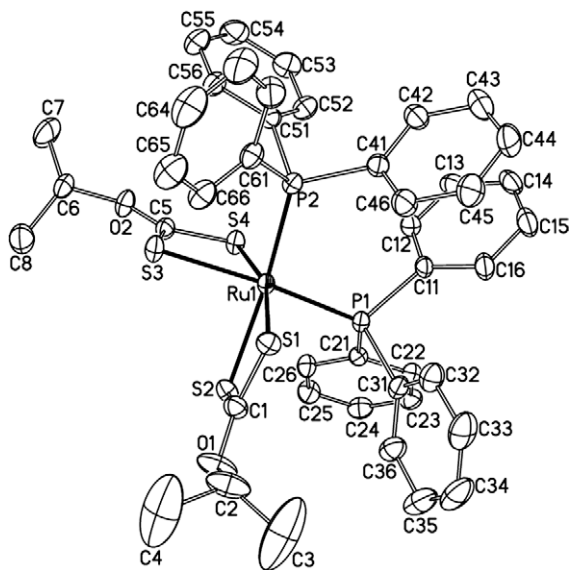


Fig. 3. Perspective view of cis - $[Ru(S_2CO^iPr)_2(PPh_3)_2]$ (**4**).

Table 3

Selected bond lengths (Å) and angles (°) for $trans$ - $[Ru(S_2CO^iPr)_2(PPh_3)_2]$ (**1**) and $trans$ - $[Ru(S_2CO^iPr)_2(PPh_3)_2]$ (**2**).

| | 2 | 3 |
|-------------------|------------|------------|
| Ru(1)–S(1) | 2.4139(9) | 2.4128(12) |
| Ru(1)–S(2) | 2.4005(10) | 2.4058(12) |
| Ru(1)–P(1) | 2.3557(9) | 2.3577(12) |
| S(1)–Ru(1)–S(2) | 108.38(4) | 108.45(4) |
| S(2)–Ru(1)–S(1)#1 | 71.62(4) | 71.55(4) |
| S(1)–Ru(1)–S(1)#1 | 180.0 | 180.00(9) |
| S(2)–Ru(1)–S(2)#1 | 180.00(4) | 180.00(6) |
| P(1)–Ru(1)–S(1) | 86.35(3) | 86.92(4) |
| P(1)–Ru(1)–S(1)#1 | 93.65(3) | 93.08(4) |
| P(1)–Ru(1)–S(2) | 88.49(3) | 86.46(4) |
| P(1)#1–Ru(1)–S(2) | 91.51(3) | 93.54(4) |
| P(1)–Ru(1)–P(1)#1 | 180.00(2) | 180.00(6) |

Symmetry transformations used to generate equivalent atoms: #1 – $x + 2$, $-y + 1$, $-z$.

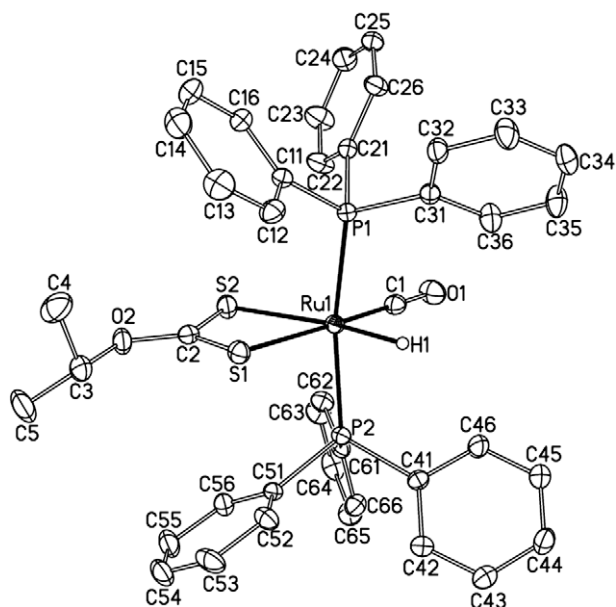


Fig. 4. Perspective view of $[RuH(CO)(S_2CO^iPr)(PPh_3)_2]$ (**6**).

Table 4

Selected bond lengths (Å) and angles (°) for cis - $[Ru(S_2COPr)_2(PPh_3)_2] \cdot CH_2Cl_2$ (**4**· CH_2Cl_2).

| | | | |
|-----------------|-----------|-----------------|-----------|
| Ru(1)–S(1) | 2.3839(7) | Ru(1)–S(2) | 2.4593(8) |
| Ru(1)–S(3) | 2.4556(7) | Ru(1)–S(4) | 2.3964(7) |
| Ru(1)–P(1) | 2.3073(7) | Ru(1)–P(2) | 2.3207(8) |
| S(1)–Ru(1)–S(2) | 71.62(3) | S(3)–Ru(1)–S(4) | 71.48(2) |
| S(1)–Ru(1)–S(3) | 95.99(3) | S(4)–Ru(1)–S(2) | 96.68(3) |
| S(3)–Ru(1)–S(2) | 88.28(3) | S(1)–Ru(1)–S(4) | 163.48(3) |
| P(1)–Ru(1)–S(1) | 94.59(3) | P(2)–Ru(1)–S(1) | 95.94(3) |
| P(1)–Ru(1)–S(4) | 96.04(3) | P(2)–Ru(1)–S(4) | 93.92(3) |
| P(2)–Ru(1)–S(3) | 86.00(3) | P(1)–Ru(1)–S(2) | 85.30(3) |
| P(1)–Ru(1)–S(3) | 165.22(3) | P(2)–Ru(1)–S(2) | 165.69(3) |
| P(1)–Ru(1)–P(2) | 103.13(3) | | |

ligands [**7**] and the $trans$ -complexes **1** (av. 2.4072(9) Å) and **2** (av. 2.4093(12) Å). The average Ru–P bond length of 2.3140(7) Å in **4**· CH_2Cl_2 agrees well with those in related ruthenium(II) complexes with PPh_3 ligands [6–17].

Similar to other 1,1-dithiolate ligands $R_2NCS_2^-$, $R_2PS_2^-$ and $(RO)_2PS_2^-$, treatment of $[RuHCl(CO)(PPh_3)_3]$ with an equimolar amount of $ROCS_2K$ in THF gave $[RuH(CO)(PPh_3)_2(S_2COR)]$ ($R = ^iPr$ **5**, tBu **6**) isolated as air-stable yellow crystals. The chloride in the starting ruthenium compound was substituted by an xanthate, and one of PPh_3 ligands was dissociated to make the ruthenium(II) center of $[RuH(CO)(PPh_3)_2(S_2COR)]$ in an octahedral coordination environment. The 1H NMR spectra of **5** and **6** display characteristic hydride resonances at δ 1.57 and 1.63 ppm, respectively [11,21]. By comparison with the ^{31}P NMR data of complexes **1–4**, the ^{31}P signals of **5** and **6** appeared as a singlet at 41.4 and 40.6 ppm, respectively, indicating that small difference for the ^{31}P signal for PPh_3 groups in these complexes is observed. The $C=O$ stretching vibration modes were found at 1935 and 1942 cm^{-1} in the IR spectra of **5** and **6**, respectively. The solid-state structure of **6** has been confirmed by X-ray crystallography. Fig. 4 shows a perspective view of **6**; selected bond lengths and angles are given in Table 5. The geometry around ruthenium is pseudo-octahedral with two $trans$ -binding PPh_3 ligands. The P–Ru–P unit is bent with an angle of 169.41(4)°. The $ROCS_2^-$ ligand chelates the ruthenium center with an average Ru–S bond length of 2.495(1) Å and the S–Ru–S angle of 70.14(4)°. The Ru–S bond lengths in **6** are longer than those in complexes **1**, **2**, and **4**· CH_2Cl_2 . The π back-bonding from the metal to the $C=O$ bond leads to elongation of Ru–S bond in **6**. The Ru–H bond length of 1.69(3) Å is within the range reported for ruthenium-hydride complexes [11,21].

Reaction of $[Ru(PPh_3)_3Cl_2]$ with tetramethylthiuram disulfide $[Me_2NCS_2]_2$ proceeded smoothly in THF solution to afford a paramagnetic dithiocarbamate complex $[Ru(PPh_3)_2(S_2CNMe_2)Cl_2] \cdot 2CH_2Cl_2$ (**7**· $2CH_2Cl_2$) in 43% yield. The reaction involved oxidation of ruthenium(II) to ruthenium(III) by the disulfide group in $[Me_2NCS_2]_2$ [27]. Complex **7** could not be obtained from the direct reaction of $[Ru(PPh_3)_3Cl_2]$ with NaS_2CNMe_2 in which no redox

Table 5

Selected bond lengths (Å) and angles (°) for $[RuH(CO)(S_2COPr^i)(PPh_3)_2]$ (**6**).

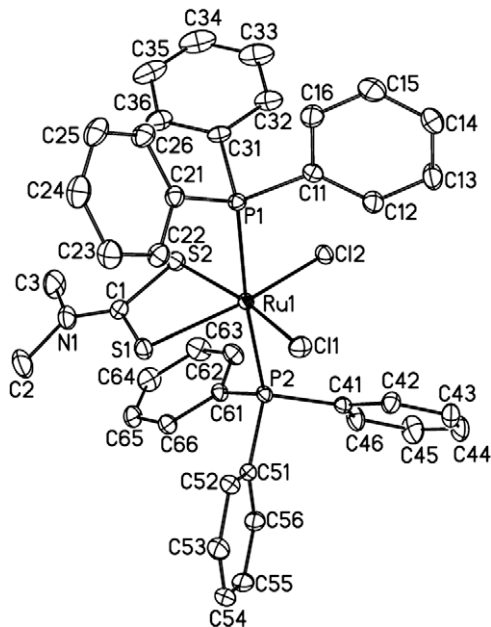
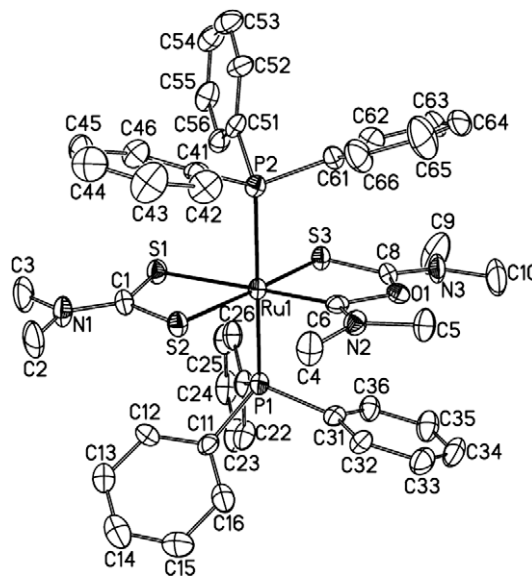
| | | | |
|-----------------|------------|-----------------|------------|
| Ru(1)–S(1) | 2.4638(12) | Ru(1)–S(2) | 2.5261(13) |
| Ru(1)–P(1) | 2.3547(12) | Ru(1)–P(2) | 2.3582(12) |
| Ru(1)–C(1) | 1.825(5) | Ru(1)–H(1) | 1.69(3) |
| S(1)–Ru(1)–S(2) | 70.14(4) | P(1)–Ru(1)–S(1) | 93.00(4) |
| P(2)–Ru(1)–S(1) | 90.08(4) | P(1)–Ru(1)–S(2) | 96.93(4) |
| P(2)–Ru(1)–S(2) | 93.65(4) | C(1)–Ru(1)–P(1) | 88.58(15) |
| C(1)–Ru(1)–P(2) | 89.23(15) | C(1)–Ru(1)–S(1) | 174.84(15) |
| C(1)–Ru(1)–S(2) | 104.80(15) | C(1)–Ru(1)–H(1) | 85.4(11) |
| P(1)–Ru(1)–H(1) | 85.1(11) | P(2)–Ru(1)–H(1) | 84.4(11) |
| S(1)–Ru(1)–H(1) | 99.6(11) | S(2)–Ru(1)–H(1) | 169.6(11) |
| P(1)–Ru(1)–P(2) | 169.41(4) | | |

Table 6Selected bond lengths (Å) and angles (°) for $[\text{Ru}(\text{PPh}_3)_2(\text{Me}_2\text{dtc})\text{Cl}_2] \cdot 2\text{CH}_2\text{Cl}_2$ ($7 \cdot 2\text{CH}_2\text{Cl}_2$).

| | | | |
|-------------------|------------|------------------|------------|
| Ru(1)–S(1) | 2.4038(10) | Ru(1)–S(2) | 2.3724(10) |
| Ru(1)–Cl(1) | 2.3795(9) | Ru(1)–Cl(2) | 2.3722(9) |
| Ru(1)–P(1) | 2.4071(9) | Ru(1)–P(2) | 2.4051(9) |
| S(2)–Ru(1)–S(1) | 71.43(3) | Cl(2)–Ru(1)–S(2) | 87.25(3) |
| Cl(2)–Ru(1)–Cl(1) | 105.31(4) | S(2)–Ru(1)–Cl(1) | 166.56(4) |
| Cl(2)–Ru(1)–S(1) | 156.30(4) | Cl(1)–Ru(1)–S(1) | 96.95(4) |
| Cl(2)–Ru(1)–P(2) | 87.93(3) | S(2)–Ru(1)–P(2) | 94.75(3) |
| Cl(1)–Ru(1)–P(2) | 90.54(3) | S(1)–Ru(1)–P(2) | 83.75(3) |
| Cl(2)–Ru(1)–P(1) | 88.14(3) | S(2)–Ru(1)–P(1) | 88.73(3) |
| Cl(1)–Ru(1)–P(1) | 86.96(3) | S(1)–Ru(1)–P(1) | 101.27(3) |
| P(2)–Ru(1)–P(1) | 174.62(3) | | |

reaction occurred. Magnetic susceptibility measurements in the solid-state showed that **7** is paramagnetic with one unpaired electron, consistent with the trivalent state of ruthenium (low-spin d^5 , $S = 1/2$) in this complex. The IR bands near 1500 and 1000 cm^{-1} for the two complexes are characteristic for the C=N (1531 cm^{-1}) and C–S (997 cm^{-1}) stretching vibration modes of the $\text{Me}_2\text{NCS}_2^-$ ligand (see Table 6).

The molecular structure of $7 \cdot 2\text{CH}_2\text{Cl}_2$, as shown in Fig. 5, was determined by single-crystal X-ray diffraction. Elemental analyses indicated the ratio of complex to the cocrystallized CH_2Cl_2 in the crystals is 1:2. The central ruthenium atom of $7 \cdot 2\text{CH}_2\text{Cl}_2$ is in an octahedral coordination environment, containing one chelated dithiocarbamate ligand, two mutually *trans* PPh_3 ligands and two mutually *cis* chlorides. The dithiocarbamate binds to ruthenium in a *S,S'*-bidentate mode, forming a four-membered ring with a $S(1)–Ru(1)–S(2)$ bite angle of 71.43(3)°. The two Ru–S bond lengths in $7 \cdot 2\text{CH}_2\text{Cl}_2$ are 2.404(1) and 2.372(1) Å, which compare well with those in the ruthenium(III/IV)–dithiocarbamate complexes such as $[\text{Ru}_3(\text{S}_2\text{CNET}_2)_6(\text{DMSO})](\text{I}_3)_2$ (DMSO = dimethyl sulfoxide) (av. 2.369(4) Å) [26], $[\text{Cp}^*\text{Ru}(\text{S}_2\text{CNMe}_2)_2][\text{N}(\text{PSPH}_2)_2]$ (av. 2.387(1) Å) [27], $[\text{Cp}^*\text{RuCl}_2\{\text{S}_2\text{P}(\text{O}^i\text{Pr})_2\}]$ (av. 2.364(1) Å) and $[\text{Cp}^*\text{RuCl}_2(\text{S}_2\text{CO}^i\text{Pr})]$ (av. 2.360(1) Å) [6] ($\text{Cp}^* = \eta\text{-C}_5\text{Me}_5$), are slightly shorter than those in ruthenium(II)–dithiocarbamate complexes such as $\text{Ru}(\text{S}_2\text{CNET}_2)_2(\text{CO}) \cdot 1/2\text{I}_2$ (av. 2.427(2) Å) [26], $\text{RuH}(\text{S}_2\text{CNMe}_2)(\text{CO})(\text{PPh}_3)_2$ (av. 2.473(1) Å), $\text{Ru}(\text{SiClPh}_2)(\text{S}_2\text{CNMe}_2)(\text{CO})(\text{PPh}_3)_2$

**Fig. 5.** Perspective view of $[\text{Ru}(\text{PPh}_3)_2(\text{S}_2\text{CNMe}_2)\text{Cl}_2]$ **7**.**Fig. 6.** Perspective view of cation $[\text{Ru}(\text{SCNMe}_2\text{OCNMe}_2)(\text{S}_2\text{CNMe}_2)(\text{PPh}_3)_2]^+$ in **8**.

(av. 2.478(1) Å) and $[\text{Cp}^*\text{Ru}(\text{S}_2\text{CNMe}_2)(\text{PPh}_3)]$ ($\text{Cp}^* = \eta\text{-C}_5\text{H}_5$) (2.399(14) Å) [28]. The average Ru–P bond length of 2.4061(9) Å in $7 \cdot 2\text{CH}_2\text{Cl}_2$ is similar to that in the ruthenium(III)– PPh_3 complex $[\text{Ru}(\text{PPh}_3)_2(\text{L})\text{Cl}_2]$ ($\text{L} = 2$ -hydroxy-acetophenone) (2.421(1) Å) [29], but longer than those in the ruthenium(II)– PPh_3 complexes such as $\text{RuH}(\text{S}_2\text{CNMe}_2)(\text{CO})(\text{PPh}_3)_2$ (av. 2.356(1) Å) [28], $[\text{Ru}\{\text{S}_2\text{P}(\text{OEt})_2\}_2(\text{PPh}_3)_2]$ (av. 2.332(1) Å) and $[\text{RuH}(\text{CO})\{\text{S}_2\text{P}(\text{OEt})_2\}(\text{PPh}_3)_2]$ (av. 2.351(1) Å) [11]. The average Ru–Cl bond length in $7 \cdot 2\text{CH}_2\text{Cl}_2$ (2.3759(9) Å) is comparable to that in the ruthenium(III) complex $[\text{Ru}(\text{PPh}_3)_2(\text{L})\text{Cl}_2]$ ($\text{L} = 2$ -hydroxy-acetophenone) (2.371(1) Å) [29], but shorter than that in the ruthenium(II) complex $[(\eta^6\text{-}p\text{-cymene})\text{RuCl}(\text{S}_2\text{CNMe}_2)]$ (2.428(1) Å) [30]. The $\text{Cl}(1)–\text{Ru}(1)–\text{Cl}(2)$ angle of 105.31(4)° in $7 \cdot 2\text{CH}_2\text{Cl}_2$ is normal for the *cis* Ru(III) dichloride compounds.

The chlorides in complex **7** are leaving groups that may easily be substituted to give new compounds. Treatment of **7** with 1 equiv. of $[\text{M}(\text{MeCN})_4][\text{ClO}_4]$ ($\text{M} = \text{Cu}, \text{Ag}$) gave the stable ruthenium(III) cationic complexes $[\text{Ru}\{\text{C}(\text{NMe}_2)\text{QC}(\text{NMe}_2)\text{S}\}(\text{S}_2\text{CNMe}_2)(\text{PPh}_3)_2][\text{ClO}_4]$ ($\text{Q} = \text{O}, \text{S}$, **8**, **9**) with ruthenium–carbon bonds. Complex **7** was converted to **8** or **9** upon treatment with the d^{10} Cu^+ or Ag^+ ion in a mixed $\text{CH}_2\text{Cl}_2/\text{MeCN}$ solvent. The reaction involved the C–S bond cleavage of $\text{Me}_2\text{NCS}_2^-$ to give the active $[\text{Me}_2\text{NCS}]^-$ species and two $[\text{Me}_2\text{NCS}]^-$ species dimerize to give a new ligand $[\text{C}(\text{NMe}_2)_2\text{S}(\text{NMe}_2)\text{S}]^-$. Of note is the formation $[\text{CH}(\text{NMe}_2)\text{OC}(\text{NMe}_2)\text{S}]^-$ due to the hydrolysis of the active $[\text{Me}_2\text{NCS}]^-$ species in a relatively long time reaction [31–33]. The measured μ_{eff} values of 1.92 μ_{B} for **8** and 1.94 μ_{B} for **9** are consistent with the ruthenium(III) formulation for both two complexes. The IR spectra of two complexes displayed a distinct $\nu(\text{Cl}=\text{O})$ band at 1095 cm^{-1} in the region expected for the $[\text{ClO}_4]^-$ anion. The IR spectra of two complexes are consistent with bidentate $\text{Me}_2\text{NCS}_2^-$ ligands, the $\nu(\text{C}=\text{N})$ and $\nu(\text{C}–\text{S})$ bands are clearly resolved and consistent with the chelated CS_2 -bound from observed in the crystallographic determination. The assignment the $\nu(\text{C}–\text{O})$ band in **8** is more problematic, due to overlap with other vibrations; a tentative assignment at 696 cm^{-1} as a strong peak is proposed. However, the $\nu(\text{C}–\text{S})$ band for C(4)–S(4) bond in the spectrum of **9** is clearly observed at 451 cm^{-1} as a sharp peak.

The solid-state structures of both complexes **8** and **9**· $2\text{CH}_2\text{Cl}_2$ have been unambiguously confirmed by X-ray crystallography. Figs. 6 and 7 show perspective views of **8** and **9**, respectively; selected bond lengths and angles of two complexes are compiled in

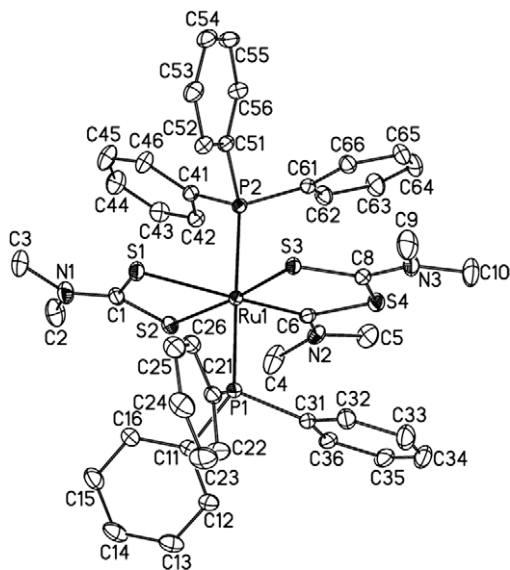


Fig. 7. Perspective view of cation $[\text{Ru}(\text{SCNMe}_2)_2(\text{S}_2\text{CNMe}_2)(\text{PPh}_3)_2]^+$ in **9**.

Table 7

Selected bond lengths (Å) and angles ($^\circ$) for $[\text{Ru}(\text{SCNMe}_2\text{OCNMe}_2)_2(\text{S}_2\text{CNMe}_2)(\text{PPh}_3)_2][\text{ClO}_4]$ (**8**) and $[\text{Ru}(\text{SCNMe}_2\text{SCNMe}_2)(\text{S}_2\text{CNMe}_2)(\text{PPh}_3)_2][\text{ClO}_4] \cdot 2\text{CH}_2\text{Cl}_2$ (**9**· $2\text{CH}_2\text{Cl}_2$).

| | 8 | 9 · $2\text{CH}_2\text{Cl}_2$ |
|-----------------|------------|--------------------------------------|
| Ru(1)–S(1) | 2.4841(14) | 2.4979(7) |
| Ru(1)–S(2) | 2.4087(13) | 2.4171(7) |
| Ru(1)–S(3) | 2.3644(14) | 2.3480(6) |
| Ru(1)–P(1) | 2.3791(15) | 2.3942(6) |
| Ru(1)–P(2) | 2.3776(15) | 2.3807(6) |
| Ru(1)–C(6) | 1.975(5) | 2.018(3) |
| S(1)–Ru(1)–S(2) | 70.39(5) | 70.28(3) |
| S(1)–Ru(1)–S(3) | 102.98(5) | 101.32(2) |
| S(2)–Ru(1)–S(3) | 172.99(5) | 171.56(2) |
| P(1)–Ru(1)–S(1) | 89.06(5) | 93.70(2) |
| P(1)–Ru(1)–S(2) | 91.52(5) | 93.82(2) |
| P(1)–Ru(1)–S(3) | 85.96(5) | 85.66(2) |
| P(2)–Ru(1)–S(1) | 88.69(5) | 84.76(2) |
| P(2)–Ru(1)–S(2) | 92.19(5) | 92.13(2) |
| P(2)–Ru(1)–S(3) | 89.92(5) | 87.91(2) |
| P(1)–Ru(1)–P(2) | 174.75(5) | 172.96(2) |
| C(6)–Ru(1)–S(3) | 82.19(17) | 87.36(8) |
| C(6)–Ru(1)–P(2) | 89.98(14) | 90.01(7) |
| C(6)–Ru(1)–P(1) | 92.69(14) | 92.55(7) |
| C(6)–Ru(1)–S(2) | 104.49(17) | 101.09(8) |
| C(6)–Ru(1)–S(1) | 174.66(17) | 169.66(8) |

Table 7 for comparison. **8** crystallized in the monoclinic system with space group $P2_1/c$, while **9**· $2\text{CH}_2\text{Cl}_2$ crystallized in the triclinic system with space group $P\bar{1}$. Two structures consist of mononuclear ruthenium complex cations and discrete $[\text{ClO}_4]^-$ anions. The $[\text{ClO}_4]^-$ anions have the expected structure as well as normal distances and angles, which will not be discussed further. The geometry at ruthenium in each of the complexes is pseudo-octahedral, given the constraints of two *trans* chelated ligands and two *trans* terminal PPh_3 ligands. The geometries of the phosphine, dithiocarbamate, and carbamatoalkyl $[\text{C}(\text{NMe}_2)\text{QC}(\text{NMe}_2)\text{S}]^-$ ($\text{Q} = \text{O}, \text{S}$) ligands and the charge of $[\text{ClO}_4]^-$ anion are as expected for ruthenium(III). The $\text{Me}_2\text{NCS}_2^-$ ligand binds to the ruthenium center with a small bite angle ($70.39(5)^\circ$ for **8** or $70.28(3)^\circ$ for **9**· $2\text{CH}_2\text{Cl}_2$), resulting in an approximately planar four-membered RuS_2P ring which contains a pair of long and short Ru–S bonds (2.4841(14) and 2.4087(13) Å for **8**, 2.4979(7) and 2.4171(7) Å for **9**· $2\text{CH}_2\text{Cl}_2$). The principal feature of interest is the metallacyclic alkyl chelate of alkylcarbamate ligand as a π -donor ligand. The five-

membered chelated metallacycles are essentially planar with deviations of 0.026 Å for **8** and 0.054 Å for **9**· $2\text{CH}_2\text{Cl}_2$ from the least-squares planes defined by Ru(1), S(3), C(8), O(1) and C(6) in **8** and Ru(1), S(3), C(8), S(4) and C(6) in **9**· $2\text{CH}_2\text{Cl}_2$, respectively. The alkylcarbamate $[\text{C}(\text{NMe}_2)\text{QC}(\text{NMe}_2)\text{S}]^-$ ligands are planar with C(4) lying 0.26 Å for **8** and 0.17 Å for **9**· $2\text{CH}_2\text{Cl}_2$ out of the least-squares planes, indicative of π donation from the sp^2 carbon to the ruthenium, which is further supported by the pattern of bond lengths within ligands: double and single bonds between C(8) and S(3) [1.698(5) Å for **8** and 1.686(3) Å for **9**· $2\text{CH}_2\text{Cl}_2$] and O(1)/S(4) [C(8)–O(1) = 1.410(6) Å for **8** and C(8)–S(4) = 1.722(3) Å for **9**· $2\text{CH}_2\text{Cl}_2$], and considerable partial double-bond character of C(6)–N(2) bond lengths (1.338(6) Å for **8** and 1.328(4) Å for **9**· $2\text{CH}_2\text{Cl}_2$). The Ru(1)–C(6) bonds at 1.975(5) Å for **8** and 2.018(3) Å for **9**· $2\text{CH}_2\text{Cl}_2$ are typical for alkyl of ruthenium(III), which are slightly longer than those in ruthenium(II)-alkyls such as $[\text{Ru}\{\text{C}(\text{C}=\text{Ph}_2)\text{SC}(\text{NMe}_2)\text{S}\}(\text{S}_2\text{CNMe}_2)(\text{CO})(\text{PPh}_3)]$ (2.148(5) Å) [32] and $[\text{Ru}\{\text{CH}(\text{C}_6\text{H}_4\text{OMe})\text{-SC}(\text{NC}_4\text{H}_2)\text{S}\}(\text{S}_2\text{CNC}_4\text{H}_8)(\text{CO})(\text{PPh}_3)]$ (2.163(5) Å) [33], but comparable to that in a ruthenium(IV) complex $[\text{RuCl}(\text{S}_2\text{CNMe}_2)(\eta^2\text{-SCNMe}_2)]$ (1.996(10) Å) [31]. The Ru(1)–S(3) dative bonds of 2.3644(14) Å in **8** or 2.3480(6) Å in **9**· $2\text{CH}_2\text{Cl}_2$ are noticeably shorter than the distances between the ruthenium and sulfur atoms of dithiocarbamate ligands, which is perhaps a reflection of the π -acidity of the *trans* dithiocarbamate ligand. The Ru(1)–S(1) (*trans* to carbon) (2.4841(14) for **8** or 2.4979(7) for **9**· $2\text{CH}_2\text{Cl}_2$) is longer than the Ru(1)–S(2) (*trans* to sulfur) (2.4087(13) for **8** or 2.4171(7) for **9**· $2\text{CH}_2\text{Cl}_2$) due to *trans* influence of the carbon atom. The average Ru–P bond lengths of **8** and **9**· $2\text{CH}_2\text{Cl}_2$ are 2.3784(15) and 2.3874(6) Å, respectively, are slightly shorter than those in the related *trans* ruthenium(III)- PPh_3 complexes such as **7**· $2\text{CH}_2\text{Cl}_2$ (2.4061(9) Å) and $[\text{Ru}(\text{PPh}_3)_2(\text{L})\text{Cl}_2]$ ($\text{L} = 2$ -hydroxy-acetophenone) (2.421(1) Å) [29]. The ruthenium atoms and two phosphorus atoms are approximately collinear, with the P–Ru–P angles deviating less than 7° from 180° .

Formal redox potentials of the ruthenium–xanthate complexes have been determined by cyclic voltammetry. The cyclic voltammograms of complexes **1–4** in CH_2Cl_2 show a reversible couple at ca. 0.13–0.16 V, vs. $\text{Cp}_2\text{Fe}^{+/0}$, which is assigned as the metal-centered $\text{Ru}^{\text{III}}\text{–Ru}^{\text{II}}$ couple because $[\text{ROCS}_2]^-$ ligand is redox inactive at this potential. The $\text{Ru}^{\text{III}}\text{–Ru}^{\text{II}}$ for **1–4** is similar to that for *cis*- $[\text{Ru}(\text{S}_2\text{CNET}_2)_2(\text{PPh}_3)_2]$ [34]. The CV of **5** or **6** shows a reversible $\text{Ru}^{\text{III}}\text{–Ru}^{\text{II}}$ couple at 0.22 V along with an irreversible oxidation wave at 0.71 V, which is tentatively attributed to $\text{Ru}^{\text{III}}\text{–Ru}^{\text{IV}}$ oxidation, which is similar to the electrochemical properties of the analogue complex $[\text{RuH}(\text{CO})\{\text{S}_2\text{P}(\text{OEt})_2\}(\text{PPh}_3)_2]$ with dithiophosphate ligand [11]. The cyclic voltammogram of **7** in CH_2Cl_2 shows two reversible couples at -0.29 V and 0.77 V vs. $\text{Cp}_2\text{Fe}^{+/0}$, which are assigned as the metal-centered $\text{Ru}^{\text{III}}\text{–Ru}^{\text{II}}$ and $\text{Ru}^{\text{III}}\text{–Ru}^{\text{IV}}$ couples, respectively. The one-electron nature of these responses has been confirmed by comparing their current heights with the standard $\text{Cp}_2\text{Fe}^{+/0}$ under identical experimental conditions. The metallacyclic complex **8** exhibits an irreversible couple at 0.28 V and a reversible couple -1.04 V, which are assigned as the $\text{Ru}^{\text{IV}}\text{–Ru}^{\text{III}}$ and $\text{Ru}^{\text{III}}\text{–Ru}^{\text{II}}$ couples, respectively. Similar couples at 0.29 V and -1.09 V were observed in the cyclic voltammetry of complex **9**. The irreversibility of Ru(III/IV) oxidation for **8** and **9** suggests that the ruthenium(III) state in these complexes is well stabilized by the combination of σ -donor phosphine and electron-rich sulfur ligands [35]. Attempts to isolate Ru(IV)–carbene complexes by oxidation of **8** or **9** with $\text{AgOSO}_2\text{CF}_3$ or $(\text{NH}_4)_2\text{Ce}(\text{NO}_3)_6$ were unsuccessful.

Acknowledgements

This project was supported by the Natural Science Foundation of China (20771003) and the Program for New Century Excellent

Talents in University of China (NCET-06-0556). Dr. Q.-F. Zhang thanks the Natural Science Foundation of the Education Bureau of Anhui Province (2006kj035a) for the assistance.

Appendix A. Supplementary material

CCDC 719648, 719649, 719650, 719651, 719652, 719653 and 722410 contain the supplementary crystallographic data for **1**, **2**, **4-CH₂Cl₂**, **6**, **7-2CH₂Cl₂**, **8**, and **9-2CH₂Cl₂**. These data can be obtained free of charge from The Cambridge Crystallographic Data Centre via www.ccdc.cam.ac.uk/data_request/cif. Supplementary data associated with this article can be found, in the online version, at doi:10.1016/j.jorganchem.2009.04.026.

References

- [1] E.I. Stiefel, ACS Symp. Ser. 653 (1996) 1. and references cited therein.
- [2] See for example: D. Sellmann, J. Sutter, Acc. Chem. Res. 30 (1997) 460.
- [3] Z. Vit, M. Zdrzil, J. Catal. 119 (1989) 1.
- [4] M.A. Bennett, M.I. Bruce, T.W. Matheson, in: G. Wilkinson, F.G.A. Stone, E.W. Abel (Eds.), Comprehensive Organometallic Chemistry, vol. 4, Pergamon Press, Oxford, 1982.
- [5] M. Schröder, T.A. Stephenson, in: G. Wilkinson, R.D. Gillard, J.A. McCleverty (Eds.), Comprehensive Coordination Chemistry, vol. 4, Pergamon Press, Oxford, 1987.
- [6] E.P.L. Tay, S.L. Kuan, W.K. Leong, L.Y. Goh, Inorg. Chem. 46 (2007) 1440.
- [7] C. O'Connor, J.D. Gilbert, G. Wilkinson, J. Chem. Soc. (A) (1969) 84.
- [8] D.J. Cole-Hamilton, T.A. Stephenson, J. Chem. Soc., Dalton Trans. (1974) 739.
- [9] D.J. Cole-Hamilton, T.A. Stephenson, J. Chem. Soc., Dalton Trans. (1977) 1260.
- [10] K. Noda, Y. Ohuchi, A. Hashimoto, M. Fujiki, S. Itoh, S. Iwatsuki, T. Noda, T. Suzuki, K. Kashiwabara, H.D. Takagi, Inorg. Chem. 45 (2006) 1349.
- [11] X. Liu, Q.F. Zhang, W.H. Leung, J. Coord. Chem. 58 (2005) 1299.
- [12] A. Pramanik, N. Bag, G.L. Lahiri, A. Charavorty, J. Chem. Soc., Dalton Trans. (1990) 3823.
- [13] M. Arroyo, S. Bernes, J. Ceron, J. Riuz, H. Torrens, Inorg. Chem. 43 (2004) 986.
- [14] N. Bag, G.K. Lahiri, A. Chakravorty, J. Chem. Soc., Dalton Trans. (1990) 1557.
- [15] A. Pramanik, N. Bag, D. Ray, G.K. Lahiri, A. Charavorty, Inorg. Chem. 30 (1991) 410.
- [16] L. Ballester, O. Esteban, A. Gutierrez, M.F. Perpignan, C. Ruiz-Valero, E. Gutierrez-Puebla, M.J. Gonzalez, Polyhedron 11 (1992) 3173.
- [17] D.J. Cole-Hamilton, T.A. Stephenson, J. Chem. Soc., Dalton Trans. (1974) 754.
- [18] W.H. Leung, K.K. Lau, Q.F. Zhang, W.T. Wong, B.Z. Tang, Organometallics 19 (2000) 2084.
- [19] Q.F. Zhang, T.Y. Lai, W.Y. Wong, W.H. Leung, Organometallics 21 (2002) 4017.
- [20] T.A. Stephenson, G. Wilkinson, J. Inorg. Nucl. Chem. 28 (1966) 945.
- [21] N. Ahmad, J.J. Levison, S.D. Robinson, M.F. Uttley, E.R. Wonchoba, G.W. Parshall, Inorg. Synth. 45 (1974) 15.
- [22] G.J. Kubas, Inorg. Synth. 28 (1996) 68.
- [23] SMART and SAINT+ for Windows NT Version 6.02a, Bruker Analytical X-ray Instruments Inc., Madison, Wisconsin, USA, 1998.
- [24] G.M. Sheldrick, SADABS, University of Göttingen, Germany, 1996.
- [25] G.M. Sheldrick, SHELXTL Software Reference Manual. Version 5.1, Bruker AXS Inc., Madison, Wisconsin, USA, 1997.
- [26] W.H. Leung, J.L.C. Chim, H. Hou, T.S.M. Hun, I.D. Williams, W.T. Wong, Inorg. Chem. 36 (1997) 4432.
- [27] W.M. Cheung, Q.F. Zhang, I.D. Williams, W.H. Leung, Inorg. Chim. Acta 359 (2006) 782.
- [28] W.H. Kwok, G.L. Lu, C.E.F. Rickard, W.R. Roper, L.J. Wright, J. Organomet. Chem. 689 (2004) 2979.
- [29] A.K. Das, S.M. Peng, S. Bhattacharya, J. Chem. Soc., Dalton Trans. (2000) 181.
- [30] W.R. Yao, Z.H. Liu, Q.F. Zhang, Acta Crystallogr. E 59 (2003) m303.
- [31] G.L. Miessler, L.H. Pignolet, Inorg. Chem. 18 (1979) 210.
- [32] B. Buriez, D.J. Cook, K.J. Harlow, A.F. Hill, T. Welton, A.J.P. White, D.J. Williams, J.D.E.T. Wilton-Ely, J. Organomet. Chem. 578 (1999) 264.
- [33] D.J. Cook, K.J. Harlow, A.F. Hill, T. Welton, A.J.P. White, D.J. Williams, New J. Chem. (1998) 311.
- [34] M. Meno, A. Pramanik, N. Bag, A. Charavorty, J. Chem. Soc., Dalton Trans. (1995) 1543.
- [35] D. Sellmass, T. Gottschalk-Gaudig, F.W. Heinemann, Inorg. Chim. Acta 209 (1998) 63.